2P5-12

Proceedings of Symposium on Ultrasonic Electronics, Vol. 37 (2016)
16-18 November, 2016

Fabrication of Bone Phantoms by 3D Printers and the Measurement of Ultrasonic Scattering

Shohei Nakata†, Chikako Kamiyama, Gen Watanabe, and Masahiro Ohno
(Chiba Institute of Technology)
中田晶平，神山真子，渡邉元，大野正弘　(千葉工大)

1. Introduction

We have been attempting to make physical bone models (phantoms) that can be used to develop the method of ultrasonic diagnosis of osteoporosis. We have previously reported[1)] the results of model-making using X-ray CT images of artificial porous materials and 3D printers. At that time, models were magnified at the printing stage because of the limited resolution of the printer, and the cortical bone was not included. In this paper, we report our attempt to make actual sized models that have both cortical and cancellous parts. We also show the experimental results of ultrasonic scattering using these models.

2. Model-making Methods and Results

2.1 Making cancellous bone models

The basic procedure to make 3-dimensional data of cancellous bone models is the same as we described in the previous report[1)]: micro X-ray CT images of polymer foam was converted to volume data by a software package *Volume Extractor* (i-Plants Systems). The BV/TV (bone volume/total volume) values were determined by setting the threshold value in this procedure.

2.2 Adding the cortical bone part

Simple-shaped cortical bone models, made of planes or bent planes, were designed with 3DCAD software (Autodesk 123Design), whereas a real-shaped cortical bone model was made from the data at the internet site *Anatomography* (DBCLS). The shape of the outer surface of a human calcaneus was downloaded from this site, then we added the inner surface to this so that the thickness became 1 mm. Cancellous bone data were filled in the inner vacancy by Boolean bonding. Models with simple-shaped cortical part were used to investigate the effect of refraction, whereas real-shaped models were used to simulate the scattering in real bones.

2.3 Actual size printing

The pore size of the polymer foam we used to mimic the cancellous part ranged 1-2 mm, which is close to the size of human cancellous bone pores. Therefore, if we can print this data together with the cortical part at the magnification of 100%, that will be an actual sized model of a human heel. We used commercial 3D printing service by Tokyo Lithmatic Corporation, which employed high resolving stereolithographic printers. Fig. 1 and Fig. 2 show the printed models. We made two cancellous bone models having different BV/TV values, 12% and 20%, and two total bone (cancellous+cortical) models with the same BV/TVs. The size of the cancellous bone models was 20×20×20 mm. The scale of the total bone model was the same as the original human data but was truncated to 23 mm.

3. Experiments of Ultrasonic Scattering

3.1 Acquiring scattered fields

Current ultrasonic bone-densitometers usually measure the sound velocity and the ultrasonic attenuation. Some researchers including us[2,3)] propose to use scattering from bones as an additional clue to determine the progress of osteoporosis, because the field distribution of scattered waves from porous materials varies by such parameters as the pore size, the trabecular thickness, and their orientation. We have performed the imaging experiment of scattered fields from the models we made. Ultrasonic tone-burst waves at 1 MHz, 2 MHz and 3 MHz, were radiated from a plane circular transducer the diameter of which was 12 mm, and the transmitted waves were visualized by hydrophone scanning. Fig. 3 and Fig. 4 show the obtained ultrasonic fields at 1 MHz and 3 MHz, respectively (results at 2 MHz being omitted).

3.2 Evaluation of the degree of scattering

Fig. 3 shows that the scattered field becomes distorted for higher BV/TV models, and at a higher frequency they become speckle-like (Fig. 4). To represent such "deforming degree" of scattering fields, we calculated autocorrelation functions of ultrasonic fields, based on the principle that the autocorrelation function becomes peaky for fast varying signals. Fig. 5 shows the values Xc, the separation of two points where autocorrelation value becomes 20% smaller than its peak. The value Xc decreased for higher BV/TV values. Fig. 6 shows profiles of autocorrelation functions for various types of models: cancellous bone only, cancellous+cortical, and cortical bone only. This experiment was done with simple-shaped models

s1673021UQ@s.chibakoudai.jp

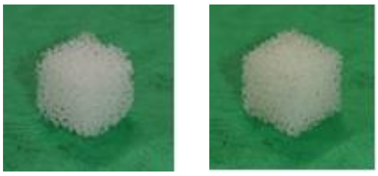

(a)BV/TV=12% (b) BV/TV=20%

Fig.1 Cancellous bone models.

(a) BV/TV=12% (b) BV/TV=20% (c) Simple-shaped model

Fig.2 Total bone models.

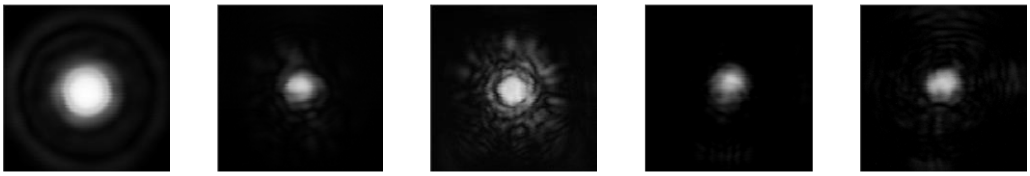

(a) water (b)Cn (12%) (c)Cn (20%) (d)Cn+ Ct (12%) (e)Cn+ Ct (20%)

Fig.3 Ultrasonic beam fields at 1 MHz. Values in parenthesis represent BV/TV.
(Cn : cancellous Ct : cortical)

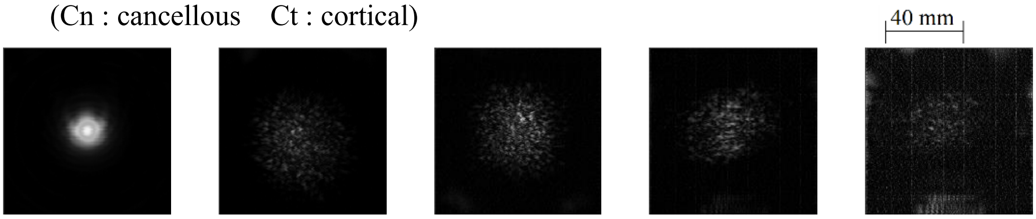

(a)water (b)Cn (12%) (c)Cn (20%) (d)Cn+Ct (12%) (e)Cn+Ct (20%)

Fig.4 Ultrasonic beam fields at 3 MHz. Values in parenthesis represent BV/TV.

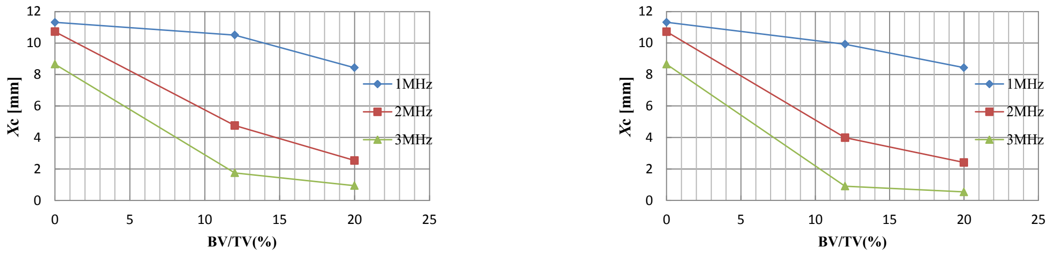

(a)Cancellous bone phantoms (b)Total bone phantoms

Fig.5 BV/TV-dependence of Xc, which is the distance between two points where autocorrelation values becomes 80% of its peak[1].

(Fig. 2(c)) with two different "bent" cortical parts (bent depth: a = 1 mm and 2 mm). The result shows that the field distortion was mainly caused by the cancellous part and the effect of the cortical part is limited.

4. Summary

We have made cancellous bone models and total bone models at an actual size using 3D printers. Ultrasonic scattering experiments show that the complexity of the scattered field, which can be evaluated by autocorrelation, can be a factor to estimate the bone density. Future work will include incorporation of more resembling cancellous bone shapes such as anisotropic or plate-like structures, and the use of materials having higher acoustic impedances.

Acknowledgment

The authors thank RIGAKU corporation for preparing X-ray data.

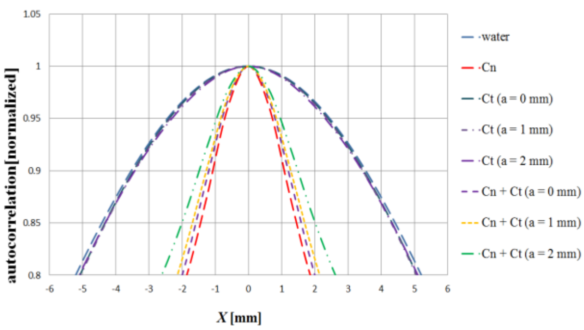

Fig.6 Autocorrelation functions for various types of model. (a : bent depth)

References

[1] M. Ohno *et.al*: Proc. of USE 2015. Vol.**36** (2015) 1P5-2.
[2] M. Ohno *et.al*: Proc. of USE 2012. Vol.**33** (2012) pp.45-46.
[3] K.A.Wear: IEEE Trans. Ultrason. Ferroelectr. Freq. Control **55** (2008) 1432.